Material Fractional Cover Algorithm

By: ASU Carbon Mapper Land and Ocean Team
Version 1.0

1. Algorithm Description

1.1. Objective

The objective of the Material Fractional Cover (MFC) algorithm is to compute the per pixel fractional coverage of selected material classes (Table 1.1) from Carbon Mapper imaging spectroscopy data by means of Multiple Endmember Spectral Mixture Analysis (MESMA), and to predict the dominant material class per image pixel. The algorithm is supposed to be extendable by custom spectral libraries and should allow for retrieving of additional semantic information beyond the class level (e.g., if a photosynthetic vegetation spectrum belongs to a tree or a shrub).

Table 1.1. List of selected material classes[1].

MaterialClass
Asphalt
Brick
Concrete
Metal
Natural Substrate
Non-photosynthetic vegetation (NPV)
Other man-made materials
Plastic
Photosynthetic Vegetation (PV)
Water

1.2 Theoretical Background

MESMA is a spectral unmixing algorithm first described by Roberts et al. (1998). It is an extension of simple Spectral Mixture Analysis (SMA) and shares the basic assumption that the spectral reflectance in a pixel can be modeled by linear combination of pure endmember reflectance spectra representing the

[1] This list was agreed on after the presentation of the development team on Oct 24, 2022.

abundant surface types weighted by their respective fractional coverage. MESMA extends SMA by enabling the number of classes and selected endmembers per class to vary on a per-pixel basis. It is a well-established algorithm and has been used in combination with case-specific spectral libraries (SLIs) for numerous different purposes including oil detection in coastal marsh lands (Petersen et al. 2015), melt pond fraction analysis on Arctic sea ice (Yackel et al. 2017), mapping of Eucalyptus subgenera (Youngentob et al. 2011), differentiating plant species within and across ecosystems (Roth et al. 2015), mapping land-cover types in a desert city (Myint and Okin 2009) and mapping spectrally similar urban materials (Wetherley et al. 2017).

Inputs to MESMA are: 1) an image to be unmixed and 2) an SLI of pure spectral endmembers associated with semantic classes of interest. For each image pixel, MESMA simulates mixed spectra using all possible combinations of spectral endmembers from different classes, along with shade fraction represented as an additional endmember of constant reflectance (see Section 1.4.3 for more detail). The combination of endmembers that results in the smallest root mean squared error (RMSE) between the simulated and the measured spectrum is retained along with their respective fractional coverage. If not specified otherwise, MESMA will always unmix a pixel spectrum with as few endmembers as possible, only selecting more complex models if the RMSE difference exceeds a user-defined threshold which is called the fusion value. In practice, this means that MESMA will first try to model each pixel spectrum with only one spectrum from the SLI and a shade fraction; this is called a two-endmember (2-EM) model. In the next step, MESMA then models each pixel spectrum as a combination of endmembers from two classes plus a shade fraction (3-EM model). A 3-EM model will only be accepted as superior to a 2-EM model if the RMSE of the 3-EM model is smaller than the RMSE of the 2-EM model by at least the fusion value. Theoretically, any level of endmember complexity is possible. Depending on data dimensionality and SLI complexity, however, higher levels are often limited by computational resources because the number of possible endmember combinations can quickly become very extensive with many spectra and classes in the SLI.

The per-pixel outputs of MESMA are 1) the endmembers resulting in the smallest RMSE, 2) the fractional coverage of the respective classes, and 3) the corresponding RMSE. In addition, MESMA may return a residual image 4) and the fractional coverage output can be translated into a hard classification 5), i.e., each pixel is assigned the class with the highest fractional coverage. See Section 2.3 for details.

1.3 Spectral Library

The SLI is a critical factor for the performance of any SMA including MESMA. It must contain representative pure spectra that cover the spectral variability for all semantic classes of interest present in a particular image. At the same time, a SLI should be as small as possible for the above-mentioned computational reasons.

SLI endmembers may either be spectra gathered with field or lab spectrometers or may be retrieved from pure image pixels, whereby adequate spatial resolution depends on the relative size of the target surfaces. The former has the virtue that pure small size samples can be acquired under controlled conditions (e.g., illumination conditions) while the latter has the advantage that system-inherent artifacts (e.g., resulting from sensor calibration or atmospheric correction) are incorporated in the data. Thus, endmembers extracted from imagery may be more appropriate for unmixing of other pixels from the same image. A

major drawback of image-based endmember extraction is that semantic information about pixels is often not available in the desired level of detail, possibly requiring time and labor-intensive field data acquisition or expert knowledge. For example, it may be easy to visually identify a pixel as a roof but challenging to identify the material it is made of.

Because a globally applicable algorithm theoretically needs to cover the vast spectral variability present in all regions of the world, we reviewed six publicly available SLIs from different regions of the world for their suitability (see Table 2.2.1 and Secs. 2.2.1 – 2.2.6 for technical details). Some SLIs are tailored to certain regions in the sense that SLI endmembers represent typical semantic classes present in the region of data collection (e.g., endmembers in the Karlsruhe Library of Urban Materials represent materials prevalent in Germany, Section 2.2.2), while others are compilations of endmembers from different regions (e.g., the ECOSTRESS Spectral Library, Section 2.2.6). Eventually, we harmonized spectra from three publicly available SLIs and enriched this compilation with spectral endmembers retrieved from visual-to-shortwave infrared (VSWIR) imaging spectroscopy data acquired with the Global Airborne Observatory (GAO) in the city of Phoenix, Arizona (Section 2.2.7). This comprehensive compiled SLI (Carbon Mapper SLI) consists of 2252 endmembers from 10 semantic classes (Table 1.1).

1.4 Spectral Library Pruning

SLI pruning is a common preprocessing step in SMA that aims to reduce the number of endmembers used for unmixing by discarding image-irrelevant and redundant spectra from the SLI, while avoiding spectral confusion. While large SLIs often contain more spectra than needed for land cover mapping of specific sites, a globally applicable algorithm with the potential to provide detailed semantic information beyond the class level to some extent contradicts the idea of SLI pruning because removal of endmembers prohibits extracting the associated higher-level information. For example, few spectra of photosynthetic vegetation may be sufficient to represent this semantic class but a specific endmember may be necessary to identify a pixel as a certain type of tree. For this reason, no SLI pruning is applied in this version of the MFC algorithm.

1.4 Assumptions and Limitations

1.4.1 Material Detection

MESMA is not initially designed as a material detection algorithm. Although under certain circumstances MESMA may have the capability to detect abundant materials on a sub-pixel scale through spectral unmixing, however it is not a detection system such as Tetracorder (Clark et al. 2003). A specific material is only detected if the corresponding endmember is part of the endmember model resulting in the smallest RMSE, i.e., its influence on the spectral mixture needs to be substantial which depends on both its fractional coverage and its spectral dissimilarity to other material classes contributing to the mixed signal. In addition, the relative influence of an endmember on the spectral mixture may be wavelength-dependent. MESMA uses all bands provided to compute the RMSE between measured and simulated spectra but some classes may be only separable (i.e., breach the pre-defined RMSE threshold) in certain wavelength regions. There are methods to optimize band selection or weighting for unmixing (e.g., Somers et al. 2009, 2010) but these approaches are based on spectral similarity of within-class

endmembers and dissimilarity of spectra between classes. This prerequisite, however, is not naturally given for many semantic classes. A generic, globally applicable approach, thus, will be limited to provide the fractional coverage of only a few dominant spectral classes in each pixel.

1.4.2 Semantic vs. Spectral Segmentation of SLIs

Semantic segmentation of the compiled SLI (Secs. 1.3, 2.2) is not based on spectral characteristics. Yet, a certain degree of inter-class separability and intra-class homogeneity is important to avoid spectral confusion, and consequently is a prerequisite for optimizing spectral band selection in SMA. For example, the class *Other man-made* is characterized by a large intra-class spectral variability across all bands which hampers application of the above-mentioned optimization algorithms.
Improved spectral segmentation of a SLI may be achieved e.g., by clustering similar spectra based on spectral distance metrics (Loughlin et al. 2020). The resulting clusters, however, may not necessarily match the desired semantic classes that users or customers are interested in.

1.4.3 Shade

In addition to a combination of one or more endmember spectra from the SLI, MESMA also fits a shade fraction during the optimization process. If not specified otherwise, shade fraction is a spectrally-uniform endmember of zero reflectance (photometric shade). Traditionally, the fractional cover of shade is allowed to vary between 0 and 0.8 (=80%) (see Table 2.2.1 for details). Yet, negative shade may be required if endmembers do not represent the brightest possible reflectance of a material and high shade fractions may enable spectral confusion, e.g., if a dark endmember can be modeled using a bright endmember with shade.
Enriching the combined SLI with image spectra required selecting spectra from bright white roofs but the selected spectra did not represent the brightest version of the associated material (Section 2.2.7). Thus, we allowed for shade to be negative (-0.1), i.e., brightening of endmember spectra and mixtures. For surfaces that are primarily distinguishable according to their brightness but not due to their spectral shape (e.g., some asphalt and concrete endmembers), however, loosening the shade constraint may enable more possible solutions of MESMA.

1.4.4 Map Grid Cell Size

Depending on the spectral complexity in a pixel, i.e., the number of classes and the degree of their spectral separability, the spatial resolution or map grid cell size impacts the performance of SMA (Wetherley et al. 2017). For large uniform landscapes consisting of very few spectrally dissimilar classes (e.g., deep dark water and bright snow in Arctic sea ice) SMA may still perform well even if grid cell size is large. Environments characterized by many small size features of partial high spectral similarity (e.g., cities) SMA is challenging. Because the number of possible endmember classes per pixel in MESMA is limited, only the spectrally most prominent classes will be reported, while surface classes with small fractional coverage or small influence on the mixed signal may not be accounted for. A particular challenge arises if the mixed spectral signal of multiple endmembers resembles the spectral shape of a pure endmember. In this case, MESMA will prefer the solution with the fewest endmembers under consideration of the fusion value if not specified otherwise (see Section 1.2).

1.4.1 Performance Assessment

Multiple criteria may be used to assess the performance of a classification model. The most frequently used performance criteria for per-class performance assessment are precision, recall and f1-score. Precision is the probability that a value in a given class was classified correctly and is mathematically defined as the ratio of values that were correctly assigned to a given class and all values assigned to the same class. It describes the model's ability to avoid false positives. Recall is the probability that a value predicted to be in a certain class really is that class, and is mathematically defined as the ratio of correctly assigned values to the sum of correctly assigned and incorrectly not unassigned values. It describes the model's ability to find all the positive samples. f1-score is the harmonic mean of precision and recall.

2. Technical Details

The MaterialFractionalCover Github repository[2] contains three iPython notebooks that include example code to run MESMA, assess classification accuracy, and harmonize the SLIs (Table 2.1). The repository further contains the harmonized SLIs in the spectral_libraries folder and its subfolders.

Table 2.1. Description of iPython notebooks in MaterialFractionalCover repository.

File	Description
spectral_unmixing.ipynb	Example implementation of MESMA. Includes helper functions for data reading, preparation and writing.
sli_harmonization.ipynb	Harmonization of SLIs for the Carbon Mapper MFC product.
accuracy_assessment.ipynb	Comparison of a high spatial resolution material classification and simulated Tanager data.

2.1 Key Dependencies

The Python version used is 3.7.13, Table 2.1.1 lists information about the used packages and the GitHub repository contains a backup of the used conda environment (conda_environment.yaml).
The foundation of the algorithm is the MESMA Python package (Crabbé et al. 2020) available on Bitbucket or the Python Package Index. The package is a translation of the original MESMA implementation in the ENVI/IDL VIPER Tools 2.0 package and also offers spectral subsetting/weighting algorithms. A comprehensive documentation and example data are available online (see Table 2.1.1). Other packages used in the iPython notebooks are Spectral Python, numpy, pandas, rasterio, xarray, rioxarray, and scikit-learn. Besides numpy, none of these libraries are requirements for MESMA.

Table 2.1.1. Used python packages.

Package	Version	Documentation	Repository	License
MESMA	1.0.8	https://mesma.readthedocs.	https://bitbucket.org/kul-	GNU General

[2] https://github.com/CMLandOcean/MaterialFractionalCover

		io/	reseco/mesma/src/master/	Public License
Spectral Python	0.22.4	http://www.spectralpython.net/	https://github.com/spectralpython/spectral	MIT
numpy	1.21.5	https://numpy.org/doc/1.21/index.html	https://github.com/numpy/numpy	BSD-3-Clause license
pandas	1.3.5	https://pandas.pydata.org/pandas-docs/version/1.3/index.html	https://github.com/pandas-dev/pandas	BSD-3-Clause license
rasterio	1.1.0	https://rasterio.readthedocs.io/en/latest/index.html	https://github.com/rasterio/rasterio	package - specific license
xarray	0.20.1	https://docs.xarray.dev/en/stable/	https://github.com/pydata/xarray	Apache-2.0
rioxarray	0.9.1	https://corteva.github.io/rioxarray/html/index.html	https://github.com/corteva/rioxarray	Unknown, Apache-2.0 licenses found
scikit-learn	1.0.2	https://scikit-learn.org/stable/index.html	https://github.com/scikit-learn/scikit-learn	BSD-3-Clause license

2.1.1 Bug Fixing

We identified a bug in the MESMA python package on line 568 in the mesma module in the core subpackage, preventing the code from returning a residual image. We changed lines 565 – 568 to the following which solved the issue:

```
565    return (np.reshape(models_expanded.T, (self.n_classes,) + image_dimensions),
566            np.reshape(fractions_expanded.T, (self.n_classes + 1,) + image_dimensions),
567            np.reshape(rmse_expanded, image_dimensions),
568            np.reshape(residuals_expanded, image.shape))
```

2.2 Input Data Requirements and Algorithm Constraints

This subsection only describes relevant details to run MESMA. An example data interface is provided in the `spectral_unmixing.ipynb` iPython notebook. MESMA requires two inputs: 1) a SLI consisting of class labels and corresponding spectra, and 2) an image with the same number of bands as the SLI. The two modules from the MESMA Python package used here are the mesma and hard_classification modules in the core subpackage.

First, an object of class MesmaModels is created using the `MesmaModels()` function from the mesma module. Then a look-up-table for all levels of complexity (by default 2-EM and 3-EM) is generated using

the `setup()` function with the class list (np.array of type str) as input. The levels of complexity to be used for MESMA can be controlled with the `select_level()` function. By default MESMA runs 2-EM and 3-EM models but it is also possible to use either one of these and higher levels of complexity can also be initiated as demonstrated in `spectral_unmixing.ipynb`.

To run MESMA, we create an object of class MesmaCore using the `MesmaCore()` function from the mesma module in the core subpackage, and use the n_cores parameter to define the number of cores dedicated to the process. Note that parallel processing is implemented through a split of the look-up-table into *n* parts defined by the n_cores parameter. For each subset of the look-up-table, a separate MESMA instance will be created. Finally, MESMA is executed using the `execute()` function of the MesmaCore object. Functions and parameters are described in more detail in Table 2.2.1.

Table 2.2.1.

Function	**Parameter**	**Description**	**Default**
`MesmaCore()`	n_cores	Number of cores dedicated to this process.	1
`execute()`	image	image to be unmixed, scaled to reflectance, without bad bands, np.array with shape (spatial_x, spatial_y, bands), needs to have the same band setting as library	NA
	library	spectral library as np.array with spectra as columns, scaled to reflectance, without bad bands, needs to have the same band setting as image	NA
	look_up_table	dict of all endmember combinations (=models) for MESMA ordered per complexity level and perclass-model (n_models × n_endmembers); output of function `return_look_up_table()` applied to MesmaModels object.	NA
	em_per_class	a dict of all library indices per endmember class; `em_per_class` attribute of MesmaModels object.	NA
	constraints	A list of length seven: 1. minimum endmember fraction, 2. maximum endmember fraction, 3. minimum shade fraction, 4. maximum shade fraction, 5. maximum RMSE,	(-0.05, 1.05, 0., 0.8,

		6. residual reflectance threshold*, 7. maximum number of consecutive bands exceeding threshold* * set value to -9999 if not used	0.025, -9999, -9999)
	no_data_pixels	tuple of indices of pixels that contain no data (result of np.where), -9999 for GAO VSWIR data	()
	shade_spectrum	single spectrum of photometric or non-photometric shade as np.array	None (=photometric shade)
	fusion_value	only select a model of higher complexity (e.g. 3-EM over 2-EM) if the RMSE is better with at least this value	0.007
	residual_image	output the residuals as an image (ignored when using band weighing or -selection)	False
	use_band_weighing	use the weighted linear spectral mixture analysis (Somers et al, 2009)	False
	use_band_selection	use the bands selection algorithm (Somers et al, 2010)	False
	bands_selection_values	tuple, correlation threshold and decrease for the band selection algorithm	(0.99, 0.01)

2.3 Outputs

The `execute()` function returns 3 or 4 arrays of shape (spatial_x, spatial_y, bands). 1) The best model where each band represents one class and the values correspond to the respective endmember IDs, 2) the model's fractions where each band contains the fractional cover of the respective class and endmember, plus the fraction of shade, 3) the model's RMSE, and 4) an optional residual image. Output values for unmodeled pixels (according to the constraints) or no data pixels are listed in Table 2.2.2.

Table 2.2.2. Output values for unmodeled or no data pixels.

	Unmodeled pixels	**No data pixels**
Models	-1	-2
Fractions	0	0

RMSE	9999	9998
Residuals image	0	0

2.4 Spectral Library Processing and Harmonization

The SLIs briefly described in Section 1.3 are characterized by different band settings and spectral coverage which needed to be aligned with the band setting of the image to be unmixed, and were converted into units of reflectance [-] in the range 0 to 1. We used the `BandResampler()` function from the Spectral Python package available on Github or the Python Package Index to resample the different band settings of the respective SLIs to match GAO and simulated Tanager data (described in Section 3.1).

Further, the classification codes of the SLIs needed to be harmonized to match the proposed material classification code in Table 1.1 (see Appendix and `sli_harmonization.ipynb` for details). This step is assumed to be a potential source of error because semantic classes may not be translated easily into one another, and endmember spectral signature is not considered for the classification (see Section 1.4). For example, the "Material" attribute *Granite with cement* may be classified as *Natural substrate* or *Concrete*. We further discarded endmembers that did not fit the proposed classification code in Table 1.1 (e.g., lichen, snow, ice).

Table 2.4.1. Publicly available SLIs investigated for their suitability.

SLI	Data source	Spectral range	Description	Included	License
Spectral Library of impervious Urban Materials	https://zenodo.org/record/4263842	400 - 2500 nm	74 samples of impervious surfaces	Yes	Mozilla Public License 2.0
Santa Barbara Urban SLI	https://ecosis.org/package/urban-reflectance-spectra-from-santa-barbara--ca	350 - 2498 nm	1065 spectra collected with an ASD around Santa Barbara, California including soil, green vegetation, non-photosynthetic vegetation and various impervious urban surfaces including roofs and paved surfaces.	Yes	-
ECOSpecLib	https://speclib.jpl.nasa.gov/	variable	> 3400 spectra of natural and man-made materials	Yes	ALL RIGHTS RESERVED Copyright California Institute of

					Technology U.S. Government Sponsorship Acknowledged under NAS CL#00-1236
Urban Material Spectral Library	https://corescholar.libraries.wright.edu/spectral_data/	450 - 950 nm	60 asphalt, brick/paver spectra	No	-
Karlsruhe Library of Urban Materials	https://www.ipf.kit.edu/english/code_1860.php; https://github.com/rebeccailehag/KLUM_library	variable	181 urban material samples, 12 material classes, and 33 material subclasses	No	GNU GPLv2
Berlin-Urban-Gradient SLI	https://dataservices.gfz-potsdam.de/enmap/showshort.php?id=escidoc:1823890	455.4 - 2446.5 nm	75 artificial and natural surface materials relevant for the study region hierarchically structured into two land cover type levels and a material description	No	Creative Commons Attribution-ShareAlike 4.0 International License

2.2.1 Urban Material Spectral Library

The Urban Material Spectral Library (UMSL; Hossler & Kelsey 2017) consists of 60 asphalt and brick/paver reflectance spectra collected around Dayton, Ohio but only covers the wavelength region between 450 and 950 nm and, therefore, was not considered in the following.

2.2.2 Karlsruhe Library of Urban Materials

The Karlsruhe Library of Urban Materials (KLUM; Ilehag et al. 2019) is an urban SLI consisting of field spectra of building materials acquired in Karlsruhe, Germany. The SLI covers the wavelength region from 350 to 2300 nm (water vapor bands around 1000, 1300 and 1800 nm are excluded) and consists of 12 classes and 33 subclasses. Although KLUM is a SLI of urban materials, some of the listed classes (e.g., Granite, Limestone, Sandstone, and Wood) are natural materials and may likewise be listed as *natural substrate*. For most of the KLUM classes, spectral variability is high, and translation into desired material classes may be hampered. For example, all metal spectra either belong to the subclasses painted metal or paint-sprayed metal. Because of the reduced number of bands, we did not use KLUM spectra here.

2.2.3 Berlin-Urban-Gradient Spectral Library

The Berlin-Urban-Gradient SLI (BUG; Okujeni et al. 2016) is a dataset for multi-scale unmixing and hard classification analyses of urban environments developed for the EnMAP mission. It consists of 75 natural and artificial surface materials relevant for the study region of Berlin, Germany. All spectra were extracted from airborne imaging spectroscopy data (HyMap, 3.6 m spatial resolution). The SLI covers the wavelength region from 455.4 to 2446.5 nm and is structured in three levels. While "Level 1" and "Level 2" hold information on land use (e.g., *Roof*), "Material name" contains information relevant for this project. Unfortunately, detailed information about the actual physical material is not provided in most cases, and the intended use of the material is described instead. For example, the material description *Brown tile* does not provide information about the actual material (e.g., concrete or metal). Other than this, spectral shape in the wavelength region around 1500 nm appears unnatural in comparison to other SLIs. For these reasons, no endmembers from BUG were used here.

2.2.4 Spectral Library of Impervious Urban Materials

The Spectral Library of impervious Urban Materials Version 1.0 (SLUM; Kotthaus 2013; Kotthaus et al. 2014) available from the London Urban Micromet data Archive (LUMA) consists of 74 material samples. Spectra were collected using an SVC HR-1024 field spectrometer and cover the wavelength region from 348.1 to 2505.8 nm. Endmembers are structured in "superclass", "class", and "material". "material", however, may include conglomerates or mixtures of two or more pure materials with regards to the list in Table 1.1. For example, the sample with the ID G002 has the "class" attribute *Granite* but the "material" is *Granite with concrete*, which itself is a mixture of the proposed material classes "natural substrate" and "concrete" in Table 1.1. Other than this, some metal samples are painted, and it is very likely that the paint pigments define the spectral reflectance, especially in the visible wavelength region. We manually extracted the relevant meta information from the PDF provided in the SLUM repository[3], then reclassified the SLUM endmembers according to Table 1.1 and stored the new class in the "MaterialClass" attribute (see Appendix and `sli_harmonization.ipynb` for details).

2.2.5 Santa Barbara Urban Spectral Library

A very comprehensive and extensively used SLI is the Urban SLI from Santa Barbara (UCSB, Herold et al. 2004) available in the Ecological Spectral Information System (EcoSIS[4]). It covers the wavelength region between 400 and 2500 nm and consists of 1065 field spectra measured with an ASD FieldSpec 3 in California. The SLI is structured in 7 levels. The associated attributes, however, often do not match the proposed list of materials in Table 1.1 but rather describe land use type or how a certain type of material has been used.

The UCSB SLI is a single csv file consisting of 1065 spectra structured in 7 levels of which the last one (Level_7) has all relevant information. We reclassified Level_7 to match the desired classification according to Table A2.1 and `sli_harmonization.ipynb` in the "MaterialClass" attribute.

[3] https://zenodo.org/record/4263842
[4] https://ecosis.org/package/urban-reflectance-spectra-from-santa-barbara--ca

2.2.6 ECOSpecLib

Another very comprehensive source is the SLI of the ECOsystem Spaceborne Thermal Radiometer Experiment on Space Station (ECOSpecLib[5]; Meerdink et al. 2019) which includes > 3400 spectra of natural and man-made materials. ECOSpecLib includes data from three other libraries (John Hopkins University, Jet Propulsion Laboratory, United States Geological Survey - Reston) and is an update of the ASTER SLI 2.0 (Baldridge et al. 2009).

ECOSpecLib is a collection of text files that had to be translated into a relational database style where each tuple consists of meta data and spectral band attributes. Spectra have been collected with different instruments and therefore have different band settings and varying spectral coverage from the visible to the thermal infrared spectral regions. We first collected all metadata in a single table and selected only those spectra that have at least one band in the wavelength region <= 450 nm. The resulting subset consists of 1947 spectra. We then excluded all spectra of "type" *Mineral* as there is no corresponding material class in the proposed list (Table 1.1) resulting in a subset of 1090 spectra.

Because the different spectral resolutions and coverages prohibit collection of spectra in a single table, we resampled all spectra to the band setting of GAO or simulated Tanager data before joining spectra with the corresponding metadata based on "Filename" as the key attribute. Based on attributes in different columns we then reclassified the SLI according to Table 1.1 (see Table A3.1) and stored the new class labels in the "MaterialClass" attribute. The corresponding code is provided in the MaterialFractionalCover Github repository in the `SLI_preparation.ipynb` notebook under the ECOSpecLib headline.

2.2.7 Spectral Library Enrichment with GAO VSWIR Data from Phoenix

Running MESMA with default settings and 2-EM models on a high spatial resolution GAO VSWIR subset from Phoenix (see Section 3 for details) revealed that not all pixels could be modeled given the provided constraints and SLI. This can have two reasons: (1) the pure pixel assumption is violated, i.e., more than one class is necessary to unmix a pixel spectrum. This is true even for the high spatial resolution data from Phoenix and may occur particularly along the edges of homogenous areas such as buildings and roads, especially if the adjacent surface is spectrally different, or in areas characterized by a natural spatial variability smaller than the spatial resolution of the data (for example park lawns may be a mixture of PV, NPV and soil), or (2) the SLI does not contain a suitable endmember. To identify the latter, we visually interpreted pixels where the RMSE threshold has been breached and used Google Imagery and Google Street View to identify materials not yet represented in the SLI by adequate endmembers. For each of the materials identified, we manually selected numerous pixels, then visually inspected the within-class spectral variability and split up classes in subclasses if within-class spectral variability was considered too large. For example, the initial class pool was split into 14 subsets representing different spectral shapes of pools. Each class consisted of at least one spectrum, and we used the mean of all spectra per subclass as the final endmember spectrum. Finally, we reclassified the extracted endmembers according to Table 1.1 and ingested them into the compiled SLI; e.g., the 14 pool endmembers representing different pool subclasses were all classified as water.

[5] https://speclib.jpl.nasa.gov/

2.2.8 Harmonization

Although attributes in the original SLIs are different, the prepared tables all contain the attributes "sli_name" (name of the originating SLI), "MaterialClass" (the semantic class according to Table 1.1), and 428 or 423 band attributes that contain the reflectance per band for the band settings of GAO and simulated Tanager data, respectively. When combining the four SLIs, we preserved the index of the original table in the attribute "original_index". ("sli_name" and "original_index") is the combined key that enables reconstructing all available information from the endmember ID in the models output of MESMA.
The final SLIs (GAO_SLI.csv and Tanager_SLI.csv in the MaterialFractionalCover Github repository) contain all attributes of the original SLIs, thus, allowing to retrieve all information provided therein including detailed semantic information beyond material class, e.g., retrieving species information from PV endmembers originating from the ECOSpecLib using the "Species" attribute.

Table with example of SLI data headers?

3. Example Data Set

Cities are a mosaic of different materials that may include all the material classes listed in Table 1.1 on small spatial scales and pose a formidable challenge for mapping MFC by means of SMA. On July 16, 2022, GAO mapped approximately 260 km^2 of the city of Phoenix, Arizona. Phoenix is a desert city which impacts the materials used in the urban environment. For example, some materials used for roads and roofs are specifically designed to reduce heat stress. It is, therefore, a good case study to test the applicability of the combined SLI consisting of spectra from different regions of the world.

In addition to testing at full resolution, we also examined the effects of running the MESMA algorithm on the GAO VSWIR data modified to mimic data from the upcoming Tanager sensors. For this, we divided the original rawspace GAO VSWIR data into a grid with an approximate 30m GSD. All IGM pixels within each grid cell were averaged to get a center location for the cell, and when applied across all grid cells this resulted in a 30m IGM. We also applied a gaussian mean filter with $\sigma = 30.0 \,/\, (2\sqrt{2log2})$ on the radiance pixel values surrounding each IGM pixel center, with weights determined by individual pixel distance from center, resulting in a matching convolved radiance map. Simulated noise was added to this radiance map using the radiometric model provided by Planet Labs PBC, and these data were processed to reflectance using the same methodology as for the full resolution image.

We used the hard classification of MESMA results on 1.05 m spatial resolution GAO VSWIR data for comparison with simulated Tanager data with a spatial resolution of 30 m of the same region. GAO VSWIR data has been atmospherically corrected with ACORN (Atmospheric CORrection Now, Analytical Imaging and Geophysics LLC) and the wavelength regions from 300 to 416 nm, 1300 to 1500 nm, 1790 to 2000 nm, and 2400 to 2600 nm corresponding to telluric water bands or not covered by some endmembers in the SLI were masked in both image and GAO SLI, respectively, resulting in 314 remaining bands. We ran MESMA with 2-EM and 3-EM models and the constraints listed in Table 4.1 using the complete GAO SLI on a 768 × 770 pixel image subset of the Phoenix data set (flightline GAO20220716t191531p0000). We then performed a hard classification on the fractions image (Figure

3.1), i.e., assigned each pixel to the class with the highest fractional coverage, and spatially resampled the classification to the grid of the simulated Tanager data assigning the mode of the classified 1.05 m pixels to the new 30 m pixels (Figure 3.2). The same wavelength mask was applied to the simulated Tanager image and Tanager SLI resulting in 312 remaining bands before we ran MESMA with identical settings (Table 3.1) on the simulated Tanager data from the same region and likewise performed a hard classification (Figure 3.3).

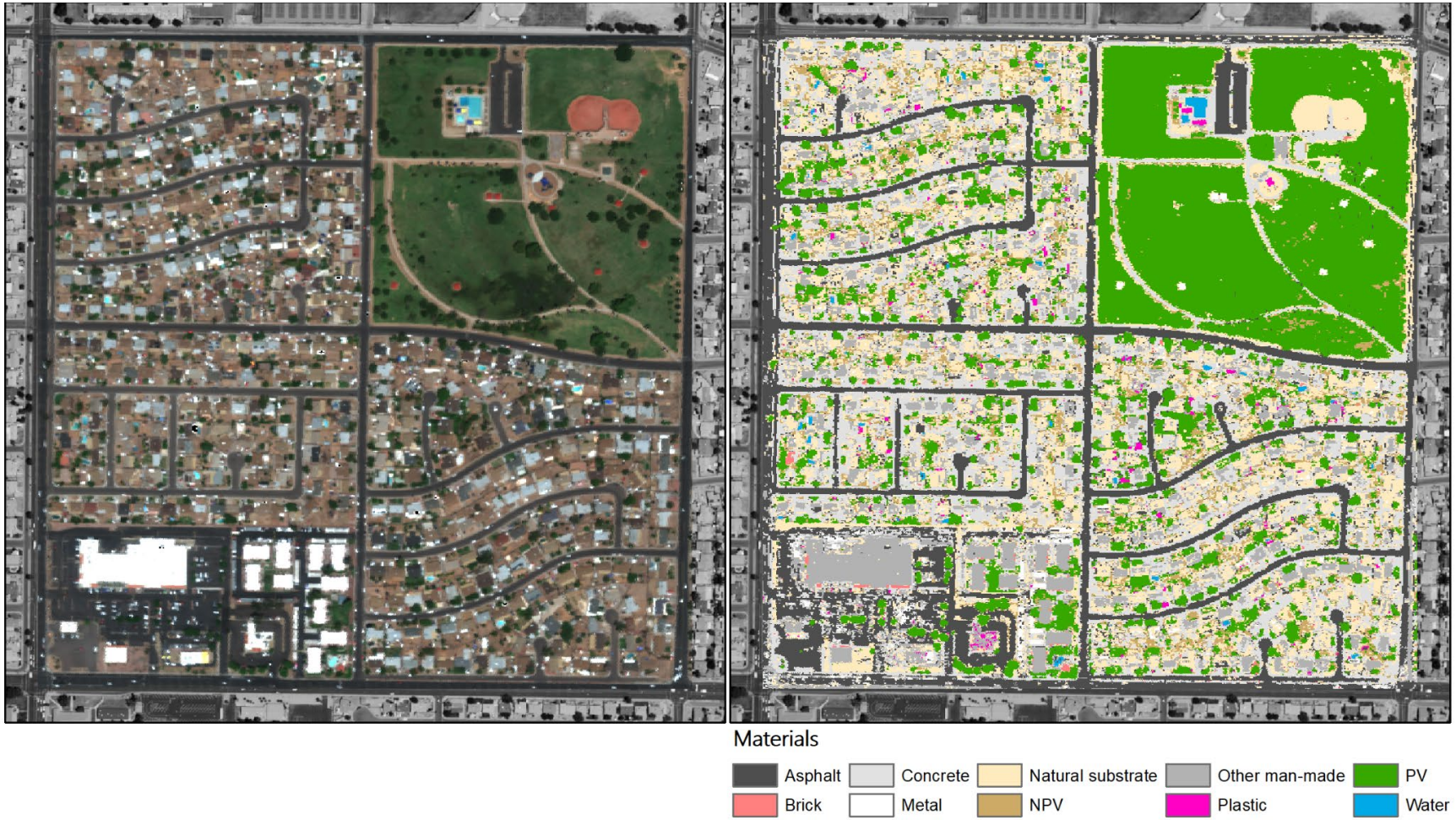

Figure 3.1. Example subset from Phoenix data set. Left: Pseudo true-color GAO imagery (1.05 m spatial resolution). Right: Hard classification of 2-EM and 3-EM MESMA fractional cover output. Background: NAIP imagery.

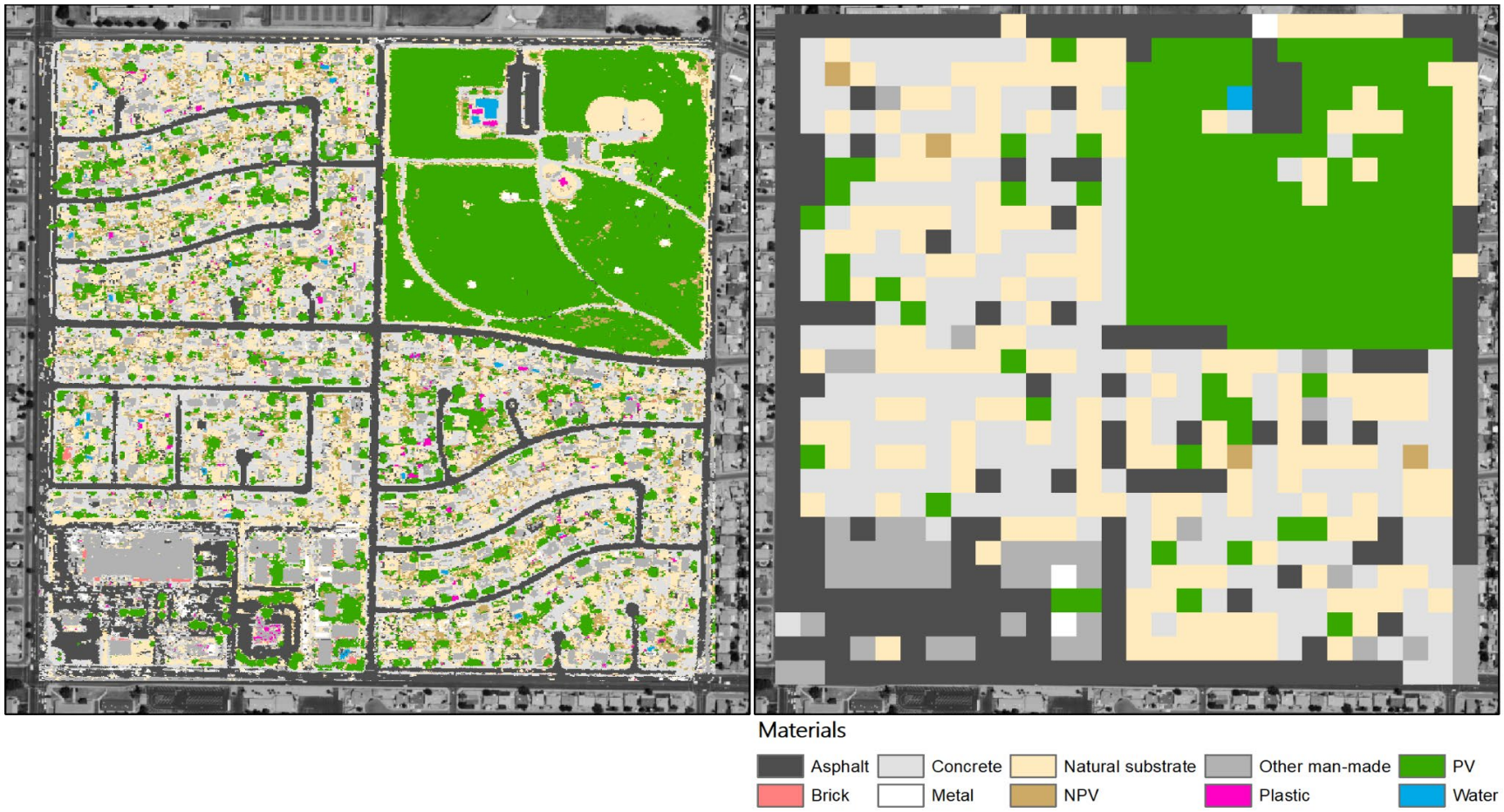

Figure 3.2. Spatial resampling. Left: Hard classification of 2-EM and 3-EM MESMA fractional cover output on 1.05 m spatial resolution GAO data (same as right panel of Figure 3.1). Right: The same hard classification resampled to the grid of simulated Tanager imagery (30 m spatial resolution) using the mode.

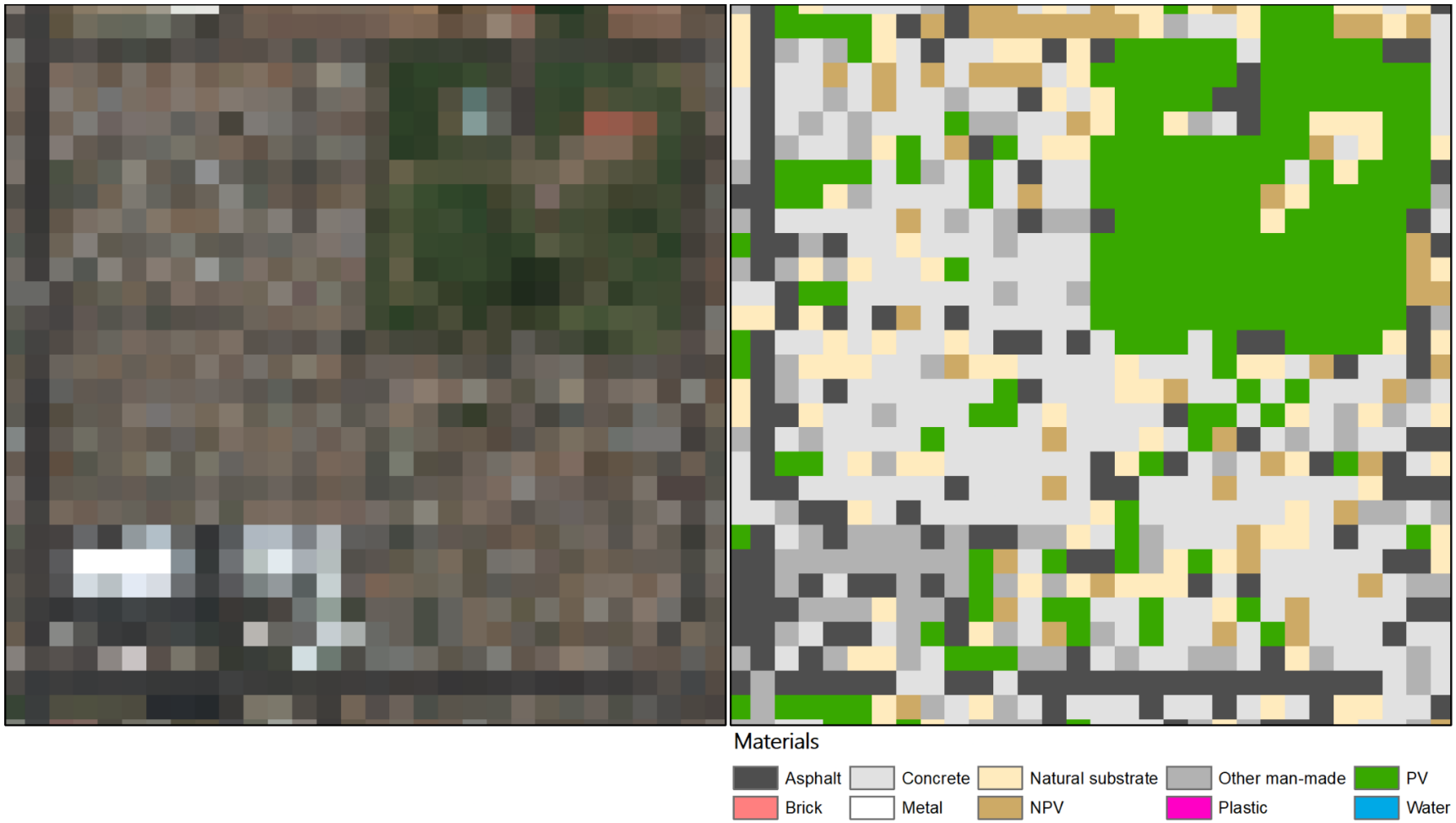

Figure 3.3. Simulated Tanager data for the same image subset from Phoenix. Left: Pseudo true-color simulated Tanager image (30 m spatial resolution). Right: Hard classification of 2-EM and 3-EM MESMA fractional cover output.

Table 3.1. Constraints used for MESMA on the Phoenix data subset (compare Table 2.1.1).

Constraint	**Value**
Minimum endmember fraction	-0.05
Maximum endmember fraction	1.05
Minimum shade fraction	-0.1
Maximum shade fraction	0.8
Residual reflectance threshold	0.05
Fusion value	0.007

4. Performance Evaluation

Performance was evaluated by computing precision, recall and f1-score for each of the classes present in the example data subset (see accuracy_assessment.ipynb) by comparing hard classification of the GAO VSWIR MESMA fractional cover output resampled to the grid of the simulated Tanager data using the mode of the classified original 1.05 m pixels inside a 30 m pixel to the hard classification of MESMA fractional cover output from the simulated Tanager data. A visual comparison is provided in Figure 4.1.

Table 4.1. Performance evaluation for example data subset. Classes not identified as dominant at 30 m spatial resolution in either data set are marked with NA.

MaterialClass	**Precision**	**Recall**	**f1-score**	**Support**
Asphalt	0.67	0.47	0.55	177
Brick	NA	NA	NA	NA
Concrete	0.52	0.66	0.58	200
Metal	0.00	0.00	0.00	3
Natural substrate	0.42	0.17	0.25	179
NPV	0.02	0.25	0.04	4
Other man-made	0.27	0.49	0.35	45
Plastic	NA	NA	NA	NA
PV	0.69	0.81	0.74	175
Water	0.00	0.00	0.00	1

Figure 4.1. Hard classification comparison. Left: Hard classification of MESMA output on simulated Tanager data (30 m spatial resolution). Right: Hard classification of MESMA output on GAO VSWIR data (1.05 m spatial resolution) resampled to simulated Tanager grid.

Literature

Baldridge, A. M., Hook, S. J., Grove, C. I., & Rivera, G. (2009). The ASTER spectral library version 2.0. Remote Sensing of Environment, 113(4), 711–715. https://doi.org/10.1016/j.rse.2008.11.007

Clark, R. N., Swayze, G. A., Livo, K. E., Kokaly, R. F., Sutley, S. J., Dalton, J. B., ... & Gent, C. A. (2003). Imaging spectroscopy: Earth and planetary remote sensing with the USGS Tetracorder and expert systems. Journal of Geophysical Research: Planets, 108(E12). https://doi.org/10.1029/2002JE001847

Crabbé, A. H., Somers, B., Roberts, D. A., Halligan, K., Dennison, P., Dudley, K. (2020a). MESMA QGIS Plugin (Version 1.0.8) [Software]. Available from https://bitbucket.org/kul-reseco/mesma.

Crabbé, A. H., Jakimow, B., Somers, B., Roberts, D. A., Halligan, K., Dennison, P., Dudley, K. (2020b). Spectral Library QGIS Plugin (Version 1.1.3) [Software]. Available from https://bitbucket.org/kul-reseco/spectral-libraries.

Herold, M., Roberts, D.A., Gardner, M.E., & Dennison, P.E. (2004). Urban Reflectance Spectra from Santa Barbara, CA. Data set. Available on-line [http://ecosis.org] from the Ecological Spectral Information System (EcoSIS)

Hossler, K., & Kelsey, S. (2017). Urban Materials Spectral Library v1.0. https://corescholar.libraries.wright.edu/spectral_data/1

Ilehag, R., Schenk, A., Huang, Y., & Hinz, S. (2019). KLUM: An Urban VNIR and SWIR Spectral Library Consisting of Building Materials. Remote Sensing, 11(18), 2149. https://doi.org/10.3390/rs11182149

Kotthaus, S. (2013). The London Urban Micromet Data Archive (LUMA) Spectral Library of impervious Urban Materials (SLUM). http://londonclimate.info/LUMA/Conditions.html

Kotthaus, S., Smith, T. E. L., Wooster, M. J., & Grimmond, C. S. B. (2014). Derivation of an urban materials spectral library through emittance and reflectance spectroscopy. ISPRS Journal of Photogrammetry and Remote Sensing, 94, 194–212. https://doi.org/10.1016/j.isprsjprs.2014.05.005

Loughlin, C., Pieper, M., Manolakis, D., Bostick, R., Weisner, A., & Cooley, T. (2020). Efficient Hyperspectral Target Detection and Identification with Large Spectral Libraries. IEEE Journal of Selected Topics in Applied Earth Observations and Remote Sensing, 13, 6019–6028. https://doi.org/10.1109/JSTARS.2020.3027155

Meerdink, S. K., Hook, S. J., Roberts, D. A., & Abbott, E. A. (2019). The ECOSTRESS spectral library version 1.0. Remote Sensing of Environment, 230 (March), 111196. https://doi.org/10.1016/j.rse.2019.05.015

Myint, S. W., & Okin, G. S. (2009). Modelling land-cover types using multiple endmember spectral mixture analysis in a desert city. International Journal of Remote Sensing, 30(9), 2237–2257. https://doi.org/10.1080/01431160802549328

Okujeni, A.; van der Linden, S.; Hostert, P. (2016): Berlin-Urban-Gradient dataset 2009 - An EnMAP Preparatory Flight Campaign (Datasets). V. 1.2. GFZ Data Services. http://doi.org/10.5880/enmap.2016.008.

Peterson, S. H., Roberts, D. A., Beland, M., Kokaly, R. F., & Ustin, S. L. (2015). Oil detection in the coastal marshes of Louisiana using MESMA applied to band subsets of AVIRIS data. Remote Sensing of Environment, 159, 222–231. https://doi.org/10.1016/j.rse.2014.12.009

Roberts, D. A., Gardner, M., Church, R., Ustin, S., Scheer, G., & Green, R. O. (1998). Mapping Chaparral in the Santa Monica Mountains Using Multiple Endmember Spectral Mixture Models. Remote Sensing of Environment, 65(3), 267–279. https://doi.org/10.1016/S0034-4257(98)00037-6

Roth, K. L., Roberts, D. A., Dennison, P. E., Alonzo, M., Peterson, S. H., & Beland, M. (2015). Differentiating plant species within and across diverse ecosystems with imaging spectroscopy. Remote Sensing of Environment, 167, 135–151. https://doi.org/10.1016/j.rse.2015.05.007

Somers, B., Delalieux, S., Stuckens, J., Verstraeten, W. W., & Coppin, P. (2009). A weighted linear spectral mixture analysis approach to address endmember variability in agricultural production systems. International Journal of Remote Sensing, 30(1), 139–147. https://doi.org/10.1080/01431160802304625

Somers, B., Delalieux, S., Verstraeten, W. W., van Aardt, J. A. N., Albrigo, G. L., & Coppin, P. (2010). An automated waveband selection technique for optimized hyperspectral mixture analysis. International Journal of Remote Sensing, 31(20), 5549–5568. https://doi.org/10.1080/01431160903311305

Wetherley, E. B., Roberts, D. A., & McFadden, J. P. (2017). Mapping spectrally similar urban materials at sub-pixel scales. Remote Sensing of Environment, 195, 170–183. https://doi.org/10.1016/j.rse.2017.04.013

Yackel, J. J., Nandan, V., Mahmud, M., Scharien, R., Kang, J. W., & Geldsetzer, T. (2017). A spectral mixture analysis approach to quantify Arctic first-year sea ice melt pond fraction using QuickBird and MODIS reflectance data. Remote Sensing of Environment, 204(September), 704–716. https://doi.org/10.1016/j.rse.2017.09.030

Youngentob, K. N., Roberts, D. A., Held, A. A., Dennison, P. E., Jia, X., & Lindenmayer, D. B. (2011). Mapping two Eucalyptus subgenera using multiple endmember spectral mixture analysis and continuum-removed imaging spectrometry data. Remote Sensing of Environment, 115(5), 1115–1128. https://doi.org/10.1016/j.rse.2010.12.012

Appendix

A1 Spectral Library of Impervious Urban Materials

Table A1.1. Classification scheme of SLUM SLI (columns 1-3) and newly assigned material.

Superclass	**Class**	**Material**	**Newly assigned material**
Asphalt	Asphalt roofing	Asphalt roofing shingle with slate chippings	Asphalt
	Road asphalt	Asphalt with stone aggregate	Asphalt
		Tarmac	Asphalt
Brick	Cement brick	Cement	Concrete
	Ceramic brick	Ceramic	Brick
		Ceramic brick	Brick
		Ceramic brick with cement	Other man-made
		Ceramic brick with paint	Other man-made
		Ceramic with cement	Other man-made
		Ceramic with paint	Other man-made
Concrete/Cement	Cement	Cement	Concrete
	Concrete	Concrete	Concrete
		Concrete with small aggregate	Concrete
		Concrete with small stone aggregate	Concrete
Granite	Granite	Granite	Natural substrate
		Granite with cement	Other man-made
Metal	Metal	Aluminium	Metal
		Aluminium plus zinc	Metal
		Aluminium, stucco	Metal
		Iron	Metal
		Lead	Metal
		Metal with paint	Metal
PVC	PVC roofing sheet	PVC	Plastic
Quartzite	Quartzite conglomerate	Quartzite	Natural substrate
Shingle	Roofing shingle	Fibre cement	Concrete
		Slate	Natural substrate
		Slate roofing shingle	Natural substrate
Stone	Stone	Carboniferous coral	Natural substrate

		limestone	
		Limestone	Natural substrate
		Sandstone	Natural substrate
Tile	Roofing tile	Cement	Concrete
		Ceramic	Other man-made

A2 Santa Barbara Urban Spectral Library

Table A2.2. Level_7 classification scheme of UCSB SLI and newly assigned material.

Level_7	**Newly assigned material**
ANNUAL_FORB	PV
ASPHALT_GRAVEL	Asphalt
ASPHALT_PARKING_LOT	Asphalt
ASPHALT_ROAD	Asphalt
ASPHALT_ROOF	Asphalt
BARK	NPV
BOUGAINVILLEA	PB
BRICK	Brick
BRICK_SIDEWALK	Brick
COMP_SHINGLE_ROOF	Other man-made
CONCRETE_BRIDGE	Concrete
CONCRETE_GRAVEL	Concrete
CONCRETE_PARKING_LOT	Concrete
CONCRETE_ROAD	Concrete
CONCRETE_SIDEWALK	Concrete
CONCRETE_TILE_ROOF	Concrete
ENGLISH_IVY	PV
GLASS_ROOF	Other man-made

GRAVEL	Natural substrate
GRAVEL_ROOF	Natural substrate
IRGR	PV
LICHEN	*EXCLUDED*
METAL_MANHOLE	Metal
METAL_ROOF	Metal
MIRRA	PV
NPV	NPV
PAINT	Other man-made
PAINTED_ROOF	Other man-made
PALM	PV
SAND	Natural substrate
SOIL	Natural substrate
STAR_JASMINE	PV
TILE_ROAD	Other man-made
TILE_ROOF	Other man-made
WOOD	NPV
WOOD_SHINGLE_ROOF	NPV

A3 ECOSTRESS

Table A3.3. Classification scheme of ECOSTRESS SLI (columns 1-4) and newly assigned material.

Type	**Class**	**Subclass**	**Name**	**Newly assigned Material**
Manmade	Concrete	Construction Concrete	Construction Concrete	Concrete
		Paving Concrete	Asphaltic concrete	Concrete
			Construction	Concrete

			Concrete	
			Construction Concrete	Concrete
	General Construction Material	Brick	Bare Red Brick	Brick
			Red smooth-faced Brick	Brick
			Weathered Red Brick	Brick
		Cement Cinderblock	Construction Concrete	Concrete
		Cinder	Cinders, ashen	Other man-made
		Glas	Plate Window Glass	Other man-made
		Marble	White Marble	Other man-made
		Paint	Black gloss paint	Other man-made
			Black paint	Other man-made
			Olive green gloss paint	Other man-made
			Olive green paint	Other man-made
		Wood	Pine Wood	NPV
	Road	Paving Asphalt	Construction Asphalt	Asphalt
		Tar	Construction Tar	Asphalt
	Roofing Material	Metal	Aluminum Metal	Metal
			Copper Metal	Metal
			Galvanized Steel Metal	Metal
			Oxidized Galvanized Steel Metal	Metal

		Roofing Paper	Black tar paper	Other man-made
		Roofing Shingle	Asphalt Shingle	Asphalt
		Rubber	Black unspecified rubber	Other man-made
			White fiberglass unspecified rubber	Other man-made
			White rubberized coating	Other man-made
		Shingle	Asphalt roofing shingle	Asphalt
			Reddish Asphalt roofing shingle	Asphalt
			Reddish asphalt Shingle	Asphalt
			Slate stone Shingle	Natural substrate
		Tile	Terra cotta Tiles	Brick
NPV	Bark	Tile	Abies concolor bark	NPV
			Acer rubrum	NPV
			Betula papyrifera	NPV
			Calocedrus decurrens bark	NPV
			Pinus coulteri bark	NPV
			Pinus lambertiana bark	NPV
			Pinus ponderosa Bark	NPV
			Pinus ponderosa bark	NPV
			Pinus strobus	NPV
			Quercus rubra	NPV

	Branches	Tile	Adenostoma fasciculatum branch	NPV
			Ceanothus megacarpus branch	NPV
			Foeniculum vulgare litter	NPV
			Salvia leucophylla 1	NPV
			Salvia leucophylla 2	NPV
			Salvia leucophylla 3	NPV
	Flowers	Tile	Calocedrus decrruens	NPV
	Leaves	Tile	Avena fatua litter	NPV
			Dry grass	NPV
			Misc Grass Litter	NPV
			Misc Grass Litter - Mostly decomposed	NPV
			Misc Leaf Litter	NPV
			Quercus sp. litter	NPV
	Lichen	Tile	dry brown lichen	*EXCLUDED*
			lichen off trees	*EXCLUDED*
	Needles	Tile	Abies concolor dry needles	NPV
			Pinus coulteri dry needles	NPV
			Pinus lambertiana dry needles	NPV
			Pinus ponderosa dry needles	NPV
PV	Grass	Chromoxerert	Avena fatua	PV

			Bromus diandrus	PV
			Grass	PV
	Shrub	Chromoxerert	Adenostoma fasciculatum 1	PV
			Adenostoma fasciculatum 2	PV
			Adenostoma fasciculatum 3	PV
			Agave attenuata	PV
			Aloe arborescens	PV
			Aloe arborescens flower	PV
			Arctostaphylos glandulosa 1	PV
			Arctostaphylos glandulosa 2	PV
			Arctostaphylos glandulosa 3	PV
			Baccharis pilularis 1	PV
			Baccharis pilularis 2	PV
			Baccharis pilularis 3	PV
			Ceanothus megacarpus 1	PV
			Ceanothus megacarpus 2	PV
			Ceanothus megacarpus 3	PV
			Ceanothus spinosus 1	PV
			Ceanothus spinosus 2	PV

			Ceanothus spinosus 3	PV
			Gasteria acinacifolia	PV
			Heteromeles arbutifolia 1	PV
			Heteromeles arbutifolia 2	PV
			Heteromeles arbutifolia 3	PV
			Juniperus chinensis	PV
			Portulacaria afra	PV
			Portulacaria afra 'Low Form'	PV
			Portulacaria afra 'Variegata'	PV
			Puya venusta	PV
			Salvia leucophylla 1	PV
			Salvia leucophylla 2	PV
			Salvia leucophylla 3	PV
			Umbellularia californica 1	PV
			Umbellularia californica 2	PV
			Umbellularia californica 3	PV
		Tile	Arctostaphylos glandulosa 4	PV
			Arctostaphylos glandulosa 5	PV
	Tree	Chromoxerert	Abies concolor 1	PV

			Abies concolor 2	PV
			Abies concolor 3	PV
			Acacia caven	PV
			Acacia visco	PV
			Acer paxii	PV
			Acer pensylvanicum	PV
			Acer rubrum	PV
			Aloe bainesii	PV
			Bambusa beecheyana	PV
			Bambusa tuldoides	PV
			Beaucarnea recurvata	PV
			Betula lenta	PV
			Betula papyrifera	PV
			Brachychiton discolor	PV
			Brachychiton rupestris	PV
			Caesalpina cacalaco	PV
			Caesalpinia cacalaco	PV
			Calocedrus decrruens 1	PV
			Calocedrus decrruens 2	PV
			Calocedrus decrruens 3	PV
			Calodendrum	PV

			capense	
			Casimiroa edulis	PV
			Cassia leptophylla	PV
			Cedrus atlantica	PV
			Cedrus atlantica 'glauca'	PV
			Cedrus deodara	PV
			Cercidium pennisulare	PV
			Chorisia insignis	PV
			Chorisia speciosa	PV
			Citharexylum montevidense	PV
			Conifer	PV
			Decidous	PV
			Ehretia austin-smithii	PV
			Eucalyptus ficifolia	PV
			Eucalyptus kartzoffiana	PV
			Eucalyptus maculata	PV
			Eucalyptus rudis	PV
			Eucalyptus rudius	PV
			Eucalyptus saligna	PV
			Fagus grandifolia	PV
			Fagus sylvatica 'atropurpurea'	PV

			Ficus craterostoma	PV
			Ficus macrophylla f. columnaris	PV
			Ficus platypoda	PV
			Ficus socotrana	PV
			Ficus thonningii	PV
			Ginkgo biloba	PV
			Ginko biloba	PV
			Hetrosideros excelsa	PV
			Jacaranda mimosifolia	PV
			Lagerstroemia indica	PV
			Macadamia integrifolia	PV
			Magnolia grandiflora	PV
			Melaleuca linariifolia	PV
			Melateuca lanceolata	PV
			Metrosideros excelsa	PV
			Olea africana	PV
			Ombu tree	PV
			Peltophorum africanum	PV
			Peltophorum dubium	PV

			Phyllostachys aurea	PV
			Phyllostachys vivax	PV
			Phytolacca dioica	PV
			Pinus lambertiana 1	PV
			Pinus lambertiana 2	PV
			Pinus lambertiana 3	PV
			Pinus ponderosa 1	PV
			Pinus ponderosa 2	PV
			Pinus ponderosa 3	PV
			Pinus strobus	PV
			Podocarpus gracilior	PV
			Prosopis articulata	PV
			Prunus serotina	PV
			Pyllostachys vivax	PV
			Quercus agrifolia	PV
			Quercus agrifolia 1	PV
			Quercus agrifolia 2	PV
			Quercus agrifolia 3	PV
			Quercus douglasii 1	PV
			Quercus douglasii 2	PV
			Quercus douglasii 3	PV
			Quercus ilex	PV
			Quercus lobata 1	PV
			Quercus lobata 2	PV

			Quercus lobata 3	PV
			Quercus robur	PV
			Quercus rubra	PV
			Quercus suber	PV
			Quercus virginana	PV
			Rubus occidentalis	PV
			Salix babylonica	PV
			Taxodium mucronatum	PV
			Tipuana tipu	PV
			Tsuga canadensis	PV
			Uvularia sessifolia	PV
Rock	Igneous	Alkalic	Hornblende Syenite	Natural substrate
			Nepheline-Sodalite Syenite	Natural substrate
			Syenite	Natural substrate
			Trachyte	Natural substrate
		Basic	Amygdaloidal Basalt	Natural substrate
			Scoria	Natural substrate
		Felsic	Alkali Granite	Natural substrate
			Alkalic Granite	Natural substrate
			Altered volcanic tuff	Natural substrate
			Aplite	Natural substrate
			Aporhyolite (felsite)	Natural substrate
			Biotite Granite	Natural substrate

			Granite	Natural substrate
			Hornblende Granite	Natural substrate
			Muscovite-Biotite Granite	Natural substrate
			Obsidian	Natural substrate
			Pegmatite	Natural substrate
			Quartz Felsite Porphyry	Natural substrate
			Rhyolite	Natural substrate
			Tuff	Natural substrate
		Feslic	Rhyolite Porphyry	Natural substrate
		Intermediate	Alkalic Syenite	Natural substrate
			Andesite Breccia	Natural substrate
			Andesite Porphyry	Natural substrate
			Augite-hypersthene Andesite	Natural substrate
			Basaltic Andesite	Natural substrate
			Diorite	Natural substrate
			Diorite Porphyry	Natural substrate
			Granodiorite	Natural substrate
			Mica Dacite Porphyry	Natural substrate
			Monzonite	Natural substrate
			Nepheline Syenite	Natural substrate
			Quartz Monzonite	Natural substrate
			Quartz Monzonite Porphyry	Natural substrate

			Rhyolitic obsidian	Natural substrate
			Tonalite (Bonsall Tonalite)	Natural substrate
		Mafic	Alkali Basalt	Natural substrate
			Anorthosite	Natural substrate
			Basalt	Natural substrate
			Basanite	Natural substrate
			Diabase	Natural substrate
			Diabase Porphyry	Natural substrate
			Gabbro	Natural substrate
			Hypersthene Gabbro	Natural substrate
			Hypersthene Gabbro (Norite)	Natural substrate
			Lamprophyre	Natural substrate
			Norite	Natural substrate
			Olivine Basalt Porphyry	Natural substrate
			Olivine Gabbro	Natural substrate
			Unaltered volcanic tuff	Natural substrate
			Vesicular Basalt	Natural substrate
		Ultramafic	Augite-Mica Peridotie	Natural substrate
			Dunite	Natural substrate
			Dunite (Olivine Peridotite)	Natural substrate
			Ijolite	Natural substrate

			Mica Peridotite	Natural substrate
			Picrite	Natural substrate
			Pyroxenite	Natural substrate
	Intermediate	Felsic	Dacite	Natural substrate
	Metamorphic	Gneis	Albite Gneiss	Natural substrate
			Augen Gneiss	Natural substrate
			Biotite Gneiss	Natural substrate
			Chloritic Gneiss	Natural substrate
			Diorite Gneiss	Natural substrate
			Felsitic Gneiss	Natural substrate
			Garnet Gneiss	Natural substrate
			Granitoid Gneiss	Natural substrate
			Hornblende Gneiss	Natural substrate
			Sillimanite-Garnet Gneiss	Natural substrate
			Syenite Gneiss	Natural substrate
		Hornfel	Banded Hornfels	Natural substrate
			Hornfels	Natural substrate
			Spotted Hornfels	Natural substrate
		Marble	Dolomite Marble	Natural substrate
			Dolomitic Marble	Natural substrate
			Marble	Natural substrate
			Pink Marble	Natural substrate
			Serpentine Marble	Natural substrate
			Verde Antique	Natural substrate

			White Marble	Natural substrate
		Phyllite	Phyllite	Natural substrate
		Quartzite	Gray Quartzite	Natural substrate
			Green Quartzite	Natural substrate
			Pink Quartzite	Natural substrate
			Purple Quartzite	Natural substrate
			Quartzite	Natural substrate
			Red Quartzite	Natural substrate
		Schist	Anthophyllite Mica Schist	Natural substrate
			Biotite Schist	Natural substrate
			Chlorite Schist	Natural substrate
			Garnetiferous Mica Schist	Natural substrate
			Graphite Schist	Natural substrate
			Green Schist	Natural substrate
			Hornblende Schist	Natural substrate
			Mica Schist	Natural substrate
			Quartz-Sericite Schist	Natural substrate
			Tourmaline Schist	Natural substrate
			Tourmaline-Mica Schist	Natural substrate
			Tremolite Schist	Natural substrate
		Serpentinite	Serpentine	Natural substrate
		Slate	Chiastolic Slate	Natural substrate
			Gray Slate	Natural substrate

			Green Slate	Natural substrate
			Red Slate	Natural substrate
	Sedimentary	Breccia	Limestone Breccia	Natural substrate
		Chemical precipitate	Gypsum	Natural substrate
			Oolitic Iron Ore	Natural substrate
		Conglomerate	Limestone Conglomerate-Breccia	Natural substrate
			Quartz Conglomerate	Natural substrate
		Dolomite	Dolomite CaMgCO3	Natural substrate
		Limestone	Argillaceous Limestone	Natural substrate
			Chalk	Natural substrate
			Cherty Limestone	Natural substrate
			Chocolate "Marble" Limestone	Natural substrate
			Dolomitic Limestone	Natural substrate
			Ecrinal Limestone	Natural substrate
			Fossiliferous Limestone	Natural substrate
			Gray Limestone (Birdseye Limestone)	Natural substrate
			Limestone	Natural substrate
			Limestone CaCO3	Natural substrate
			Lithographic Limestone	Natural substrate

			Oolitic Limestone	Natural substrate
			Travertine (Calcareous Tufa)	Natural substrate
		Sandstone	Argillaceous Sandstone	Natural substrate
			Arkose	Natural substrate
			Arkosic Sandstone	Natural substrate
			Ferruginous Sandstone	Natural substrate
			Glauconitic Sandstone	Natural substrate
			Gray Sandstone	Natural substrate
			Greywacke Sandstone	Natural substrate
			Micaceous Sandstone (Brownstone)	Natural substrate
			Purple-banded Sandstone	Natural substrate
			Red Sandstone	Natural substrate
			Sandstone (Flagstone)	Natural substrate
			Sandstone (Micaceous Red)	Natural substrate
			Sandstone (Red)	Natural substrate
		Shale	Arenaceous Shale	Natural substrate
			Argillaceous Shale	Natural substrate
			Black Shale	Natural substrate
			Calcareous Shale	Natural substrate
			Carbonaceous Shale	Natural substrate

			Illite-bearing Shale	Natural substrate
			Oil Shale (Kerogen Shale)	Natural substrate
			Phosphorite	Natural substrate
			Shale (Arenaceous)	Natural substrate
			Shale (Calcareous)	Natural substrate
			Shale (Phosphatic)	Natural substrate
		Siliceou	Diatomaceous Earth	Natural substrate
			Siliceous Oolite	Natural substrate
		Siltstone	Limestone Siltstone	Natural substrate
			Limestone-Siltstone	Natural substrate
			Siltstone	Natural substrate
		Travertine	Travertine	Natural substrate
		dolomite	Dolomite $CaMgCO_3$	Natural substrate
Soil	Alfisol	Fragiboralf	Pale brown silty loam	Natural substrate
		Haploxeralf	Brown to dark brown gravelly loam	Natural substrate
		Haplustalf	Brown fine sandy loam	Natural substrate
			Brown loamy fine sand	Natural substrate
		Paleustalf	Brown sandy loam	Natural substrate
			Dark reddish brown fine sandy loam	Natural substrate
			Reddish brown fine sandy loam	Natural substrate

	Aridisol	Calciorthid	Light yellowish brown interior dry gravelly loam	Natural substrate
			Light yellowish brown loam	Natural substrate
		Camborthid	Brown silty loam	Natural substrate
			Light yellowish brown loamy sand	Natural substrate
		Gypsiorthid	Very pale brown to brownish yellow interior dry gravelly silt loam	Natural substrate
		Haplargid	Brown gravelly sandy loam	Natural substrate
		Salorthid	Dark brown interior moist clay loam	Natural substrate
			Dark yellowish brown silty clay	Natural substrate
			Light yellowish brown clay	Natural substrate
		Torripsamment	Very dark grayish brown loamy sand	Natural substrate
	Entisol	Quartzipsamment	Brown to dark brown sand	Natural substrate
		Torripsamment	White gypsum dune sand.	Natural substrate
		Ustifluvent	Brown to dark brown silt loam	Natural substrate
	Inceptisol	Cryumbrept	Gray/dark brown extremely stoney coarse sandy	Natural substrate
		Dystrochrept	Dark yellowish brown micaceous loam	Natural substrate

		Haplumbrept	Brown sandy loam	Natural substrate
			Dark brown fine sandy loam	Natural substrate
		Plaggept	Very dark grayish brown silty loam	Natural substrate
		Ustocrept	Pale brown dry silty clay loam	Natural substrate
		Xerumbrept	Brown to dark brown gravelly fine sandy loam	Natural substrate
	Mollisol	Agialboll	Dark grayish brown silty loam	Natural substrate
		Agriudoll	Vary dark grayish brown loam	Natural substrate
		Argiustoll	Very dark grayish brown silty loam	Natural substrate
		Cryoboroll	Black loam	Natural substrate
			Very dark grayish brown loam	Natural substrate
		Haplaquoll	Gray silty clay	Natural substrate
		Hapludoll	Brown to dark brown sandy loam	Natural substrate
		Haplustall	Grayish brown loam	Natural substrate
		Paleustoll	Very dark grayish brown loam	Natural substrate
	Spodosol	Cryohumod	Dark reddish brown, organic-rich, silty loam	Natural substrate
	Utisol	Hapludult	Brown to dark brown loamy sand	Natural substrate
	Vertisol	Chromoxerert	Brown to dark brown clay	Natural substrate

Water	Frost	none	Frost	*EXCLUDED*
	Ice	none	Ice	*EXCLUDED*
	Snow	Coarse Granular	Coarse Granular Snow	*EXCLUDED*
		Fine Granular	Fine Snow	*EXCLUDED*
		Medium Granular	Medium Granular Snow	*EXCLUDED*
	Tap Water	none	Tap water	Water